Design of a PIV objective maximizing the image signal-to-noise ratio

Olivier Chételat   Kyung Chun Kim

School of Mechanical Engineering, Pusan National University
Pusan 609–735, Korea (South)

Abstract

PIV (particle image velocimetry) systems use a camera to take snapshots of particles carried by a fluid at some precise instants. Signal processing methods are then used to compute the flow velocity field. In this paper, the *design of the camera objective* (optics) is addressed. The optimization is done in order to maximize the signal-to-noise ratio of in-focus particles. Four different kinds of noise are considered: photon shot noise, thermal and read noise, background glow shot noise, and noise made by the other particles. A semi-empirical model for the lens aberrations of a two-doublet objective is first addressed, since further, it is shown that lens aberrations (low f-value $f_\#$) should be used instead of the Fraunhofer diffraction (high f-value) for the fitting of the particle image size with the pixel size. Other important conclusions of the paper include the expression of optimum values for the magnification M, for the exposure period τ and for the pixel size ξ.

1 Introduction

Particle image velocimetry (PIV) is a technique for measuring the velocity field of gas or liquids. The field is usually limited to a planar subspace (2D) and the velocity is described by vectors lying in this plane (2D). However, 3D/2D PIV (multi-plane PIV) and 3D/3D PIV (stereo and holographic PIV) are also possible.

The idea of PIV is to observe particles carried by the flow to measure. The particles should be small enough to faithfully follow the flow velocity variations, but big enough to be seen by a camera. Indeed, a strobe light (or sometimes the camera shutter) is used to take snapshots of the particle positions at different instants. The light is usually shaped (for 2D/2D PIV) in a light sheet that defines the measurement plane. Image processing techniques can then compute the velocity field (and possibly other fields like rotational, divergence, acceleration, etc.). The flow may naturally contain particles, e.g., dust or pollen for air flows, bubbles or plankton for water flows, or may be artificially seeded with, e.g., oil droplets for gas, hollow glass balls for liquids. An overview of modern PIV as well as other similar non-invasive optical techniques for flow velocity measurements can be found in [6, 10].

The camera objective used in PIV applications is not optimized with the same criteria as for usual imaging cameras. The latter is designed to take "good snapshots," which generally means high resolution of highly luminous and contrasted pictures of objects in a plane, with acceptable diminution of these performances within a zone, on both sides of this plane, defined by the *depth of field*.

Alternatively and more generally, "good snapshots" can be defined as pictures with a high signal-to-noise ratio. However, what is the part of the signal and noise of a picture is application dependent. The "signal" is the information the end user (a human being, or a computer) would like to "see" in an ideal perfect world in order to fulfill its need, and the "noise" is what conceals part of this information.

For a PIV system, the signal is, according to [1], the *center position* of *identified particles* at *known instants*. Other approaches take into account the convolution process usually used to compute the velocity field [8, 13]. In PIV applications, there is no specific need to have a good "portrait" of the particle: a particle image may be fuzzy, as long as its center position is preserved. For the same reason, in PIV applications, the classical definition of the *depth of field* has also to be revised. To avoid confusions, [11] speaks of *measurement depth* and [13] introduces the notion of *particle visibility*.

The origins of noise are various and numerous. For example, the irregular shape of the particles (that can rotate in its 3D world between two pictures) may introduce an error in the determination of the particle

center. Other noise examples include the optical aberrations of the objective, the diffraction of the light (speckles), the Brownian motion of the particles (for the emerging PIV applications using sub-micron particles), the optical shot noise, and the optical-electronic noise of the camera (or of the film, for film-based PIV). Two other important sources of noise come from projection errors of out-of-focus particles (central projection of usual objectives, also called perspective) and from the overlapping of other particle images, especially for high particle density and/or in the case of volume illumination.

A camera objective (i.e., optics) usually contains many lenses (or possibly mirrors) in order to reduce its noise (which is assumed to be mainly the lens aberrations, responsible for blurred images, and the unwanted reflections at the lens interfaces and objective walls, responsible for poorly contrasted images). Some special lens arrangements can even correct the projection errors mentioned above by replacing the usual central projection with an orthogonal projection (telecentricity) [12]. However, the more lenses used, the more attenuation of the light, since no lens is totally transparent and reflection free (appropriate lens coating can however significantly reduce reflections).

To get the more light possible, the aperture of the objective should be chosen high, i.e., low f-values $f_\#$ (or, equivalently, high numerical aperture NA). More light is advisory since the strobe light period can be shorter (which allows the system to measure faster flows), or the size and price of the illumination system can be reduced. For a given objective type, lower f-values however considerably increase the lens aberrations [9, 15]. Actually, as discussed further in the paper, the size of a particle image roughly grows with $1/f_\#^3$ for low f-values with the consequence that the spot area increases with $1/f_\#^6$. On the other hand, the light power going through the objective increases only with $1/f_\#^2$. This results in a *lower* light density on the sensor, and thus a lower signal per pixel. However, the size of the sensor pixels may be taken larger to fit the wider spot (either physically, or by signal processing). This however diminishes the resolution potential of the camera, which may be unwanted, since it reduces the product DSR $\times$ DVR ("Dynamic Spatial Range" times "Dynamic Velocity Range") known to be a quality index for PIV cameras [1].

Additionally or alternatively, the maximal exposure period (defined by an acceptable blur caused by the particle motion) can be longer for larger particle images with the consequence of increasing the sensor signal. However, larger particle images also have the effect of increasing the "apparent particle concentration", which is responsible for additional noise, and may finally result in a lower signal-to-noise ratio. The problem with PIV objectives is that many effects have to be taken into account in order to obtain the truth to the question "What is the best f-value to chose?", since simple models usually lead to contradictory answers (as just discussed).

To completely answer this question, the lens aberrations should be taken into account. However, the lens aberration models are usually difficult to derive and in the PIV literature, lens aberrations are usually just mentioned, or in the best case, an expression is given for an objective comprising one plano-convex lens only [15]. When the particle image has to be enlarged, the published solutions recommend to increase the magnification M, or the f-value to take advantage of the Fraunhofer diffraction [1]. However, another alternative may be to *decrease* the f-value and therefore using the lens aberrations. This paper investigates this other option.

Besides, the PIV literature has just begun to consider some PIV setups with "volume illumination" [11, 13]. For this kind of illumination, the "noise made by the other particles" has somehow to be included in the optimization process. In this paper, we try and systematically take into account the most relevant factors that influence the signal-to-noise ratio to finally optimize the camera objective.

The camera objective will be assumed of a given type, and the optimization will only deal with the three objective parameters s (the distance to the in-focus plane), M (the magnification) and especially $f_\#$ (the f-value). As for lens aberrations exact analytical models of objectives do not exist, we will derive our conclusions from approximate models obtained empirically from ray tracing simulations. The chosen objective type in this paper is made of two cemented doublets and constitutes a simple example for more complex objectives.

2 Particle image size

2.1 Ideal objective

Object points are characterized by their intensity I and their 3D-coordinates $(p_x, p_y, s + \zeta)$. They are *out-of-focus* when $\zeta \neq 0$ and *in-focus* when $\zeta = 0$. In the latter case, they define a plane approximately the distance s away from the objective.

Point images are homogeneously luminous discs with center (c_x, c_y) and diameter D, and are lighted with the flux Φ going through the objective. According to geometrical optics, the mapping that applies luminous points onto point images is

$$c_x = M \frac{s}{s+\zeta} p_x \qquad c_y = M \frac{s}{s+\zeta} p_y \tag{1}$$

$$D = M \frac{Ms}{f_\#(1+M)(s+\zeta)} |\zeta| \qquad \Phi = \left[\frac{Ms}{f_\#(1+M)(s+\zeta)} \right]^2 I \tag{2}$$

The three constants s, M (magnification) and $f_\#$ (f-value), in addition to the above equations, completely specify an *ideal objective* [9]. An ideal objective neither takes into account the wave nature of light (diffraction) nor the lens aberrations. Moreover, the projection is central (perspective).

The central projection has also the effect to change the apparent concentration of particles (the field of view is wider for distant particles). For a uniform volume concentration C, the apparent concentration C' is

$$C' = \left[\frac{s+\zeta}{Ms} \right]^2 C \tag{3}$$

Ideal telecentric objectives [12] have the equations (1) and (3) replaced by

$$c_x = Mp_x \qquad c_y = Mp_y \qquad C' = \frac{C}{M^2} \tag{4}$$

which is what would be obtained with an orthogonal projection. However, equation (2) still depend on ζ: a telecentric objective does *not* prevent out-of-focus points to get fuzzy.

A normalized disc may also be described by a probability-like *distribution* (i.e., probability density function or PDF)

$$f_i(x,y) = \begin{cases} 1/2\pi\sigma_i^2 & \text{for } x^2 + y^2 \le 2\sigma_i^2 \\ 0 & \text{otherwise} \end{cases} \tag{5}$$

with, as an alternative measure of the disc size, the standard deviation

$$\sigma_i = \frac{D}{2\sqrt{2}} \tag{6}$$

2.2 Lens aberrations

Two parabolic surfaces (mirrors or lenses) are perfect for imaging one point only. Even worse, no point at all can be perfectly imaged with spherical surfaces. Nevertheless, spherical surfaces are much easier to manufacture than any other surface and several spherical lenses can significantly reduce the *lens aberrations* [9]. This is the reason why most of lenses have spherical surfaces. However, no finite set of lenses (of any shape) can make up an ideal objective.

The third order theory of lens aberrations results in the so-called *Siedel sum* which comprises five terms [9]. The first term only depends on $1/f_\#^3$ and stands for what is commonly called the *spherical aberrations*. The *coma* is the second term with a dependence on $1/f_\#^2$ and h/s, where h is the off-axis distance of a luminous point at the in-focus plane. The third term models the *astigmatism* with $1/f_\#$ and $(h/s)^2$. The *curvature of field* is the fourth term and also depends on $1/f_\#$ and $(h/s)^2$. Finally, the fifth term, the *distortion*, is function of h/s only. Another aberration comes from the different colors of light and for this reason is called *chromatic aberration*. However, the relatively monochromatic laser light usually used for PIV results in much smaller chromatic aberration than what one is accustomed to have with anthropocentric imaging applications. ·

Lens aberrations are easy to simulate using the *ray tracing* method, which simply applies geometrical optics to a bundle of rays. Ray tracing does not classify the aberrations like the third order theory does: all aberrations of any kind are automatically taken into account. However, the results are valid only for one specific value of $(h, s, M, f_\#)$. As the analytical derivation of aberration expressions is very tedious (and anyway approximative), in this paper a semi-empirical approach has been chosen: when analytical models
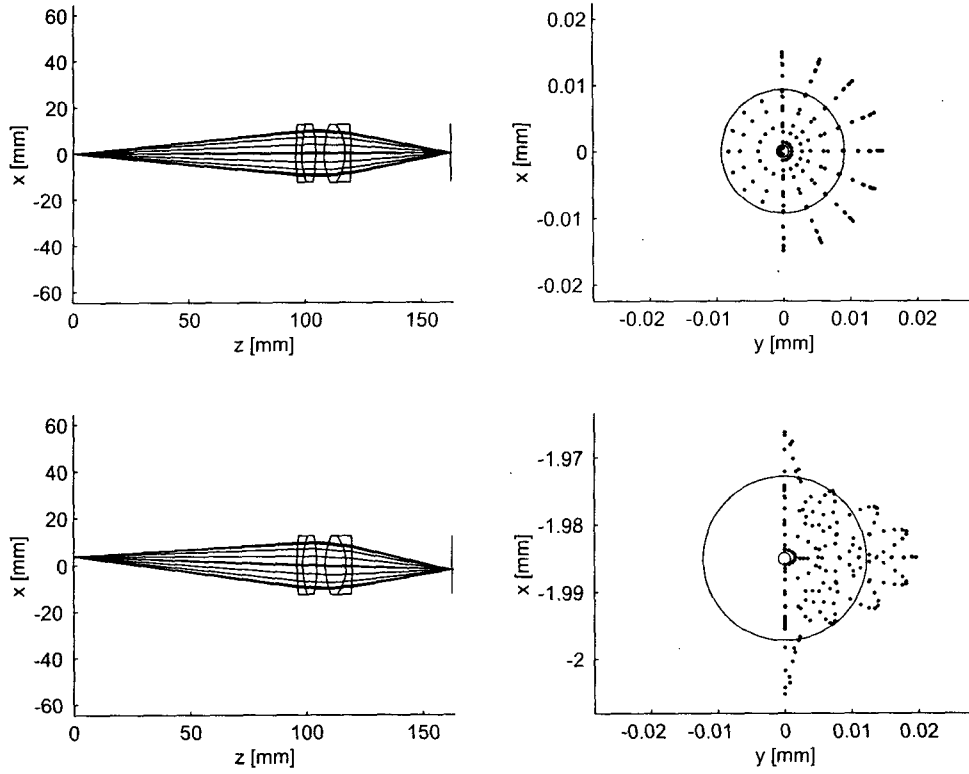
Figure 1: Ray tracing of a simple two doublet objective. This objective was used in a MPIV (miniature PIV) system developed by the authors [3, 4]. The upper row of sub-figures is for the off-axis point ($h = 0$) and the lower row is for the most off-axis point ($h = 4$ mm) that still has its image on the camera sensor.

are too difficult to derive, empirical models that fit the results of many ray tracing simulations are seek. This method is simple, general, quick and accurate.

In the PIV literature, lens aberration models are very rare and remain very basic. In [15] is mentioned an analytically derived expression for *spherical aberrations* of a single *plano-convex lens*. However, a practical objective would be composed of more than one lens and only very cheap objectives would use plano-convex lenses. Figure 1 presents a ray tracing simulation of a more realistic objective composed of two cemented doublets (achromats). This type of objective was actually used for a MPIV (miniature PIV) system developed by the authors and described in [3, 4]. The sub-figure of the upper left corner shows, as an example, some of the simulated rays for an on-axis point ($h = 0$). In the upper right corner is the section of the simulated rays for the "best-focused" object point (definition in next paragraph). Since the objective has a rotation symmetry, only rays for $y \geq 0$ are simulated; observe however that this does not prevent the most external rays to intersect the image plane at $y < 0$. The lower left and right corners show similar simulations performed for the "most" off-axis point ($h \gg 0$).

An object point is *best-focused* when the size of its image spot is the less spread. A reasonable measure of the size of the image spot is the standard deviation (or inertia circle) of the swarm of points obtained with a ray tracing simulation. A higher weight is given to outer rays, since they subtend a wider solid angle. With σ_a as the size of the particle image due to lens aberrations, one has, for N rays

$$\mu_x = \frac{\sum_{i=1}^{N} \theta_i x_i}{\sum_{i=1}^{N} \theta_i} \qquad \mu_y = \frac{\sum_{i=1}^{N} \theta_i y_i}{\sum_{i=1}^{N} \theta_i} \tag{7}$$

126

$$\sigma_{\mathrm{a}} = \sqrt{\frac{\sum_{i=1}^{N} \theta_i x_i^2}{\sum_{i=1}^{N} \theta_i} - \mu_x^2 + \frac{\sum_{i=1}^{N} \theta_i y_i^2}{\sum_{i=1}^{N} \theta_i} - \mu_y^2} \tag{8}$$

where θ_i is the angle between the optical axis and the ray i at the object point.

The camera sensor is usually planar, but the best-focused surface (defined by all best-focused points that have their image at the sensor plane) is not planar because of the *curvature of field*. This aberration does not allow any objective to perfectly map an object plane to an image plane: at least one of them is not exactly planar. In the ray tracing simulation, the best-focused points have to be searched iteratively (e.g., dichotomy search) since they are generally slightly off the in-focus plane defined by the ideal objective model.

Both *curvature of field* and *distortion* can be obtained by ray tracing or by calibration of a physical objective. Therefore, the effect of these aberrations in a PIV context can be taken into account and corrected when processing the velocity field. In other words, to *optimize* the objective of a PIV system, the only thing that really matters is the *spot* of the best-focused points (size and possibly shape). The exact position of the best-focused points projected onto the in-focus plane (x-, y-coordinates), or normal to this plane (z-coordinate) are not relevant at this stage.

The spot of one best-focused point (size and shape) can be fully modeled by a distribution $f_{\mathrm{a}}(x, y)$. For a given objective, there is a different distribution f_{a} for every best-focused point. However, since objectives generally have a rotation symmetry, all points at the same distance h from the axis share the same distribution.

Fortunately, a too fine model for the *shape* of f_{a} is generally not necessary since f_{a} is finally convolved with many other contributions with the result of smoothing out the details [as we shall see at (16)]. The most relevant information contained in the distribution f_{a} is its standard deviation σ_{a} (the big circles in Figure 1 have their radius equal to σ_{a}). The standard deviation σ_{a} still depends on h.

For quasi paraxial rays (h small), the doublet aberrations is approximately constant. With the assumption $h = 0$, one obtains the following empirical model [5]

$$\sigma_{\mathrm{a}} = K_{\mathrm{a}} \frac{M s \sqrt{1 + M^6}}{f_{\#}^3 (1 + M)^3} \tag{9}$$

where $K_{\mathrm{a}} = 0.0033$ for standard cemented doublets.

The image of an object point which takes into account the lens aberrations has a distribution f approximately given by the convolution

$$f = f_{\mathrm{a}} * f_{\mathrm{i}} \tag{10}$$

This expression is exact for in-focus points (since f_{i} is a Dirac distribution) and for points much out-of-focus (since f_{a} is then negligible). For in-between points, it is a fair approximation (but is not exact, since both f_{a} and f_{i} use the geometrical optics laws and are not totally independent). With this assumption (10), the standard deviation is

$$\sigma = \sqrt{\sigma_{\mathrm{a}}^2 + \sigma_{\mathrm{i}}^2} \tag{11}$$

2.3 Fraunhofer diffraction

In the previous subsection, the images have been computed based on geometrical optics. However, the light emitted by an in-focus object point *diffracts* through the circular aperture of a real objective, which results in an image described by the Airy function [11, 9]

$$f_{\mathrm{F}}(r) = \left\lceil \frac{2 J_1(v)}{v} \right\rceil^2 \qquad v \approx \frac{\pi r}{\lambda f_{\#}(1 + M)} \tag{12}$$

where λ is the light wave length, J_1 a Bessel function of the first kind, and r the radial coordinate ($r = \sqrt{x^2 + y^2}$). This expression is derived for an in-focus object point on the optical axis, but can be used as a fairly good approximation for off-axis points or for out-of-focus points (if convolved with f_{i}). See [11] for an exact expression.

As the Airy function slowly decreases, the standard deviation is infinite and cannot be used as a measure of its expanse. Instead, the usual measure for the Airy function expanse is given by the radius of its first

zero [15, 9]. However, such a measure is not compatible with the other contributions to the particle image size: the sum of the square is no longer possible. To overcome this difficulty, the solution generally adopted [2] is to approximate the Airy function by a (2D) Gaussian which, at zero, shares the same value, slope and curvature

$$f_F(r) \approx e^{-r^2/\sigma_F^2} \qquad \sigma_F = \frac{2\lambda f_\#(1+M)}{\pi} \qquad (13)$$

2.4 Particle size

A particle reflects or scatters light depending on its size and on the wave length of the light used. The light scattered by two points of the particle is generally not independent in phase, which makes modeling very difficult. Moreover, the particle can be sufficiently transparent for the light to partially go inside and to reflect many times with the surface. See [14] for a study of the particle image according to the Generalized Lorenz-Mie theory.

The problem can be greatly simplified if one assumes that the particles are *self-luminous* (independence of phase and with a Lambert emission, i.e., isotropic emission). This assumption generally means that the interferences are not modeled. However, if fluorescence is involved [13], as the incident photons are re-emitted with a random phase or with another wavelength, there is truly no interference possible. In the other case, the assumption can be justified like for the lens aberrations: since many function f are finally convolved together, the "details" of the shape are smoothed out. Only the standard deviation really matters.

A self-luminous sphere is seen as an homogeneously-luminous disc (like the sun or the moon), which means that the distribution f_p is similar to (5). Therefore, the standard deviation σ_p is

$$\sigma_p = \frac{Md}{2\sqrt{2}} \qquad (14)$$

where d is the diameter of the particle.

The convolution of f_p with the other contributions is exact with the self-luminous assumption.

2.5 Sensor pixel

The camera sensor (CMOS or CCD) consists in an array of photosensitive pixels. The numerical values the camera provides are the integration of the light over the exposure period τ and over the pixel sensitive area. The spatial integration means that the camera sensor actually samples the image convolved with the pixel sensitive area, instead of simply sampling the photo-image.

The *pixel area* is a square of size ξ containing the sensitive area plus the electronics accessing the pixel (which does not take part in the light integration). To simplify the modeling, let us assume that the *sensitive area* is a disc of diameter $c\xi$, with a *fill factor* $c < 1$. This disc can be described by a distribution f_c similar to (5). The standard deviation σ_c is

$$\sigma_c = \frac{c\xi}{2\sqrt{2}} \qquad (15)$$

2.6 Immobile particle

The image of a particle in an immobile fluid can therefore be modeled by its distribution f that takes into account the size of the particle, the camera resolution and the camera objective, which includes the geometrical optics, the lens aberrations and the Fraunhofer diffraction

$$f = f_0 * f_i \qquad f_0 = f_c * f_p * f_F * f_a \qquad (16)$$

where f_0 is the in-focus part. For particle much out-of-focus, f will be approximately equal to f_i (which is a disc) since f_0 is negligible. For in-focus particle, f_i vanishes, but the exact distribution of f_0 is not known. However, a Gaussian distribution is usually considered as a sensible approximation, since f_0 is the result of many convolutions. With comparable standard deviations, the convolution of many functions tends rapidly towards a Gaussian function (limit central theorem). In any case, the standard deviation $\sigma(\zeta)$ of f is

$$\sigma(\zeta) = \sqrt{\sigma_0^2 + \sigma_i^2(\zeta)} \qquad \sigma_0 = \sqrt{\sigma_c^2 + \sigma_p^2 + \sigma_F^2 + \sigma_a^2} \qquad (17)$$

where σ_0 is the in-focus part.

2.7 Mobile particle

The longer is the exposure time τ, the more light is collected by the sensor. However, if τ is too large with respect to the particle velocity v, the particle image will change to a path, i.e., the image of the particle trajectory.

If a mathematical point were the image of a particle moving at constant velocity v, the image would be, for the whole exposure period τ, a line segment of length $Mv\tau$. The standard deviation σ_τ of such a segment is

$$\sigma_\tau = \frac{Mv\tau}{2\sqrt{3}} \tag{18}$$

Thus, the standard deviations of a real particle image in the displacement direction and in the transverse direction are

$$\sigma_{\parallel} = \sqrt{\sigma_\tau^2 + \frac{\sigma^2}{2}} \qquad \sigma_{\perp} = \frac{\sigma}{\sqrt{2}} \tag{19}$$

3 Signal

3.1 Pixel size

For a signal to be properly sampled, the Shannon-Nyquist theorem requires that the sampling frequency be higher than twice the signal highest frequency. The highest frequencies are for the most narrow section of the particle images, i.e., for the transverse section of the path made by an in-focus particle (i.e., described by $\sigma_\perp$). If the intensity function of this section is assumed Gaussian, i.e., in proportion to $\exp(-t^2/2\sigma_\perp^2)$ (where t is the transverse coordinate), then its spectrum is in proportion to $\exp(-2\pi^2\sigma_\perp^2 f^2)$, where f is the frequency. In other words, the spectrum of the $\sigma_\perp$ Gaussian is still a Gaussian, but with standard deviation $1/2\pi\sigma_\perp$. One can assume that a Gaussian is negligible beyond an arbitrary multiplicity β of its standard deviation (β is usually chosen around 3, but for PIV, it is acceptable (and sometimes better) to use lower values, e.g., $\sqrt{3}$ according to [16]). Thus, the sampling period is expressed by

$$\xi = \frac{\pi}{\beta}\sigma_\perp \tag{20}$$

Usually, the sampling period is given (for example, by the specific technology of the camera), and the objective has to be designed accordingly [1]. Thus, for a given ξ, one should have

$$\sigma_0(s, M, f_\#) = \frac{\beta\sqrt{2}}{\pi}\xi \tag{21}$$

This constitutes the first equation. Two others are needed to uniquely define the objective parameters s, M and $f_\#$.

For very high f-values, the Fraunhofer diffraction are dominant. Thus,

$$\frac{\beta\sqrt{2}}{\pi}\xi = \sigma_0 \approx \sigma_F = \frac{2\lambda f_\#(1 + M)}{\pi} \tag{22}$$

and, solving this equation for $f_\#$

$$f_\# = \frac{\beta\xi}{\sqrt{2}\lambda(1 + M)} \tag{23}$$

On the other hand, for very low f-values, the lens aberrations are dominant, and one has

$$\frac{\beta\sqrt{2}}{\pi}\xi = \sigma_0 \approx \sigma_a = K_a \frac{Ms\sqrt{1 + M^6}}{f_\#^3(1 + M)^3} \tag{24}$$

i.e.,

$$f_\# = \left[\frac{\pi K_a Ms\sqrt{1 + M^6}}{\sqrt{2}(1 + M)^3\beta\xi}\right]^{1/3} \tag{25}$$

3.2 Exposure period

The longer the exposure period τ, the higher is the camera signal. However, as the particles are moving, a too long exposure transforms the particle images to traces with the main undesirable effect of increasing the "noise" caused by neighbor particles (that more frequently overlap).

However, even if one consider an isolated particle, the maximum intensity of the particle trace is already reached after a short displacement of the particle. With the Gaussian assumption of the in-focus particle images, one can again consider the Gaussian distribution null beyond $\beta\sigma_\perp$. Therefore, the intensity of the particle trace is maximum for a particle displacement of $2\beta\sigma_\perp$. Thus, there is no gain to use exposure periods τ longer than

$$\tau_{\max} = \frac{\sqrt{2}\beta}{Mv}\sigma_0 = \frac{2\beta^2}{\pi Mv}\xi \tag{26}$$

where v is the particle velocity. The corresponding σ_τ is $\beta\sigma_0/\sqrt{6}$.

The exposure period τ_{opt} that gives the best signal-to-noise ratio has to be optimized in consideration of the influence of the other particles [see (49)].

3.3 Signal

The signal of a particle image can be estimated by integrating the average light over the pixel area ($\pi c^2\xi^2/4$) and over the exposure period τ. The average light is defined to be the light flux Φ entering the objective divided by the "particle image area" more or less arbitrarily assumed to be $2\pi\sigma_\perp\sigma_\parallel$ (ellipse surface at the standard deviation "radius").

$$S = \frac{\tau c^2\xi^2}{8\sigma_\perp\sigma_\parallel}\left[\frac{Ms}{f_\#(1+M)(s+\zeta)}\right]^2 I \tag{27}$$

For in-focus particles, one obtains

$$S_0 = \frac{\sqrt{3}\pi^2\xi\tau I c^2 M^2}{4\beta f_\#^2(1+M)^2\sqrt{\pi^2 M^2 v^2\tau^2 + 12\beta^2\xi^2}} \tag{28}$$

and for much out-of-focus particles ($\sigma \approx \sigma_i$)

$$S_i = \frac{2\tau c^2\xi^2 I}{M^2\zeta^2} \tag{29}$$

4 Noise

4.1 Photon shot noise

Any photo-sensor has a fundamental noise caused by the discrete nature of photons [7]. The variance of this noise is in proportion to the optical signal. Thus, the noise standard deviation is

$$N_{\mathrm{ph}} = K_{\mathrm{ph}}\sqrt{S} \tag{30}$$

where K_{ph} is a constant.

4.2 Thermal and read noise

CMOS or CCD camera are electronic devices and are subject to thermal noise $\sqrt{4kTB}$, where B is the bandwidth and k the Bolzmann constant [7]. In a camera, this noise is integrated over the exposure period τ and over the pixel area $\pi c^2\xi^2/4$, i.e., the noise is in proportion to $\sqrt{\pi c^2 kTB\tau\xi^2}$. As the bandwidth B for an integration over τ is $1/\tau$, the thermal noise is

$$N_{\mathrm{th}} = K_{\mathrm{th}}c\xi\sqrt{kT} \tag{31}$$

where K_{th} is a constant.

In a CMOS or CCD camera, the thermal noise also introduces a charge uncertainty when the pixel capacities are reset. Even though the origin of this noise is thermal, the so-called *read noise* is usually considered as an independent source of noise, because the means used to reduce it are specific. However, in our study, its formulation is identical to the other sources of thermal noise (as described above).

4.3 Noise made by the other particles

The noise caused by other particles is very important in PIV applications, especially for high particle concentration or volume illumination. However, its formulation is difficult, since it depends for a large part on the ability of the PIV algorithm to identify a given particle [1]. Figure 2 shows simulations performed for an increasing width $\Delta\zeta$ of the light sheet. The particles are idealized in the sense that they are perfectly spherical and all of the same size. The objective follows the ideal objective model and the particle images are assumed to be Gaussian. Every image is normalized with respect to its maximum and minimum intensity, except for a zone in the upper left corner of each image which is kept with the absolute intensity, i.e., with the *same* "gain" for every image.

The noise due to overlapping is indeed low for thin light sheets. Subjectively, one can decide that the noise is acceptable up to $\Delta\zeta \approx 1.6$ mm in the example of Figure 2. For thicker light sheet, many particles overlap and errors in the particle identification and localization are to be expected, especially for the most out-of-focus particles. From $\Delta\zeta \approx 50$ mm, even the in-focus particles are difficult to extract, since the "background glow" reaches a very high intensity.

A given particle is "difficult to identify and localize" if, at the particle position, the other particles substantially contribute to the image intensity. Thus, an important step in the formalization of the "noise made by the other particles" is achieved with the statistics of the image intensity.

The probability to have, at a given pixel (x, y) of the image, an intensity H resulting from a *unique particle*, anywhere in a *given* object plane (ζ given), is described by a probability density function $h_1(H)$. The random variable H has the following average and variance

$$\mu_1 = \frac{\pi c^2 \xi^2}{4} \tau \frac{\Phi}{A} * f \qquad \nu_1 = \frac{\pi^2 c^4 \xi^4}{16} \tau^2 \frac{\Phi^2}{A} * f^2 - \mu_1^2 \tag{32}$$

where A is the area in which the particles are confined. The convolution with the constants Φ/A and Φ^2/A actually performs the average of Φf, respectively $(\Phi f)^2$. At first, it could look strange to use a convolution to evaluate an average. However, this is the correct expression for non homogeneous illumination, i.e., when Φ depends on (x, y).

In practice, the concentration C of particles is not high enough for the particles to significantly disturb each other (the volume taken by the particles is negligible with respect to the fluid volume). Consequently, the distribution h_1 for a given particle can be assumed unchanged if the particle is isolated or surrounded by other particles.

The number $\mathrm{d}N$ of particles in a given plane and confined in the area A is

$$\mathrm{d}N = AC'\mathrm{d}\zeta = \left\lceil \frac{s + \zeta}{Ms} \right\rceil^2 AC\mathrm{d}\zeta \tag{33}$$

At a given point (x, y) of the camera sensor, the intensity is the sum of the contribution due to these $\mathrm{d}N$ particles described by the *same* probability distribution h_1. Thus, the distribution of the intensity tends to a *Gaussian distribution*, whatever is the distribution h_1 (central limit theorem), with average

$$\mathrm{d}\mu = \mu_1 \mathrm{d}N = \frac{\pi c^2 \xi^2}{4} \tau C \left\lceil \frac{1}{f_\#(1 + M)} \right\rceil^2 (I * f)\mathrm{d}\zeta \tag{34}$$

and variance (with $A \to \infty$)

$$\mathrm{d}\nu = \nu_1 \mathrm{d}N = \frac{\pi^2 c^4 \xi^4}{16} \tau^2 C \left\lceil \frac{Ms}{f_\#^2(1 + M)^2(s + \zeta)} \right\rceil^2 (I^2 * f^2)\mathrm{d}\zeta \tag{35}$$

The particles illuminated by a transversal, infinitesimally thin, light sheet have the same ζ and the same illumination intensity I. As in this case the expression $I * f = I(f * 1) = I$ holds for *any* distribution f, the average illumination is the general expression

$$\mathrm{d}\mu = \frac{\pi c^2 \xi^2}{4} \tau I C \left\lceil \frac{1}{f_\#(1 + M)} \right\rceil^2 \mathrm{d}\zeta \tag{36}$$

The variance however depends on the distribution f, but by chance, $1 * f^2$ is equal to $1/2\pi\sigma^2$ for a disc *or* a Gaussian distribution. Thus, for in-focus particles, one obtains, with the assumption that f_0 is a Gaussian

$\Delta\zeta = 0.16\,\mathrm{mm}$ $\Delta\zeta = 0.28\,\mathrm{mm}$ $\Delta\zeta = 0.5\,\mathrm{mm}$

$\Delta\zeta = 0.89\,\mathrm{mm}$ $\Delta\zeta = 1.6\,\mathrm{mm}$ $\Delta\zeta = 2.8\,\mathrm{mm}$

$\Delta\zeta = 5.0\,\mathrm{mm}$ $\Delta\zeta = 8.9\,\mathrm{mm}$ $\Delta\zeta = 16\,\mathrm{mm}$

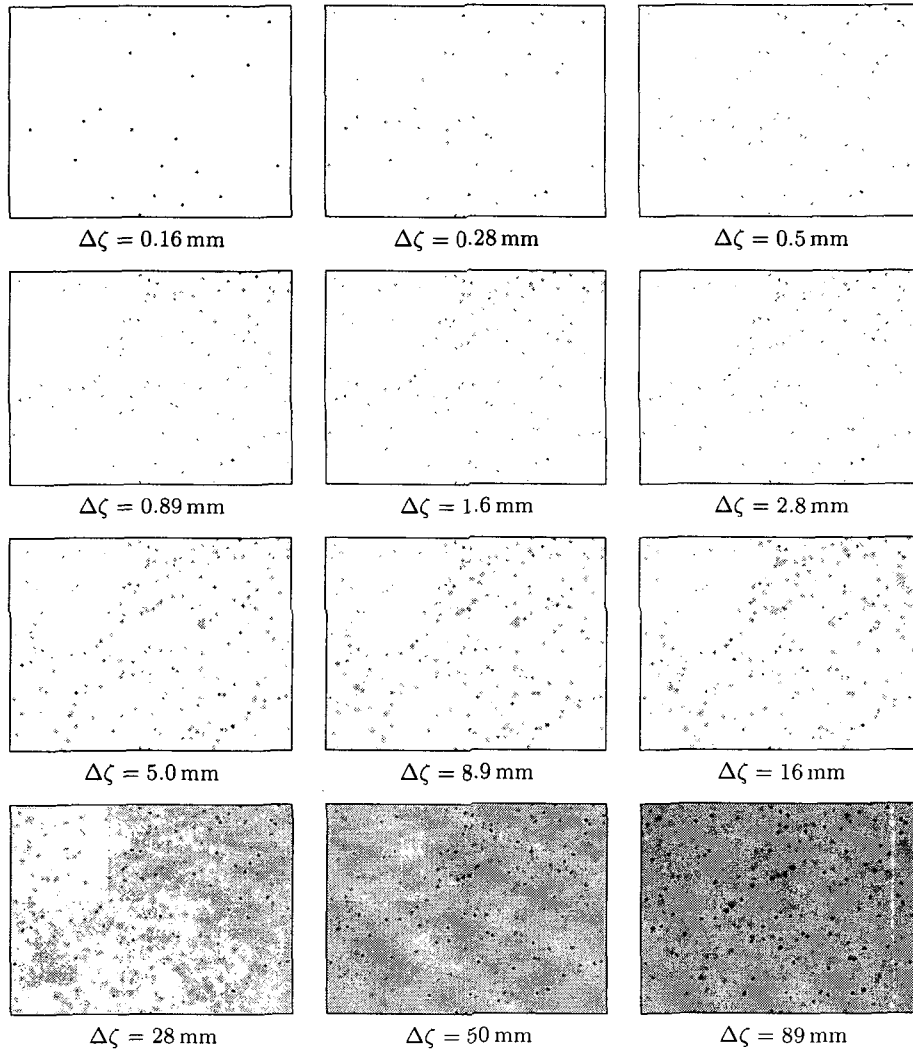$\Delta\zeta = 28\,\mathrm{mm}$ $\Delta\zeta = 50\,\mathrm{mm}$ $\Delta\zeta = 89\,\mathrm{mm}$

Figure 2: Typical pictures obtained with increasing light sheet thickness (simulation). White corresponds to obscurity and black to the maximum of light got in the picture, except in the upper left corner of the pictures where black corresponds to the maximum of light got in picture $\Delta\zeta = 89$ mm (this for absolute intensity comparison between pictures). General parameters are $s = 100$ mm, $f_\# = 1.9$, $M = 0.5$, $\sigma_0 = 12\,\mu$m, $C = 5/\mathrm{mm}^3$, observation area is 6.4 mm × 4.8 mm, $\zeta_b = -\zeta_a$.

or a disc

$$d\nu_0 = \frac{\pi c^4 \xi^4 \tau^2 C I^2}{32\sigma_0^2} \left[\frac{M}{f_\#^2 (1+M)^2} \right]^2 d\zeta \tag{37}$$

and, for much out-of-focus particles

$$d\nu_i = \frac{\pi c^4 \xi^4 \tau^2 I^2 C}{4} \left[\frac{1}{f_\#(1+M)M\zeta} \right]^2 d\zeta \tag{38}$$

There is even a close expression for any ζ

$$d\nu \approx \frac{\pi c^4 \xi^4 \tau^2 I^2 C}{4} \left[\frac{M}{f_\#(1+M)} \right]^2 \frac{d\zeta}{M^4\zeta^2 + 8\sigma_0^2 f_\#^2 (1+M)^2} \tag{39}$$

where the very reasonable assumption $s \gg \sigma_0$ was taken into account to simplify the expression.

The light sheet used in a classical PIV is usually thin, but not infinitesimal. Thus, the correct expressions have to be integrated over the "thickness" of the light sheet. The resulting average is still valid for any distribution f

$$\mu = \frac{\pi c^2 \xi^2 \tau I C \Delta\zeta}{4 f_\#^2 (1+M)^2} \tag{40}$$

where $\Delta\zeta$ is the thickness of the light sheet.

The variance can be obtained in a close form only with the Gaussian/disc assumption

$$\nu = \frac{\pi c^4 \xi^4 \tau^2 I^2 C}{16\sqrt{2}\sigma_0 f_\#^3 (1+M)^3} \left[\arctan \frac{M^2\zeta_a}{2\sqrt{2}\sigma_0 f_\#(1+M)} - \arctan \frac{M^2\zeta_b}{2\sqrt{2}\sigma_0 f_\#(1+M)} \right] \tag{41}$$

where ζ_a and ζ_b define the boundary of the light sheet.

Illumination with a very thick light sheet turns into what is called *volume illumination* [11, 13]. In volume illumination, the function arctan of the variance (41) may tend to its asymptotes at $\pm\pi/2$. In this case, the variance is reduced to

$$\nu < \frac{\pi^2 c^4 \xi^4 \tau^2 I^2 C}{16\sqrt{2}\sigma_0 f_\#^3 (1+M)^3} \tag{42}$$

Observe that the variance for a "symmetric" thick light sheet ($\zeta_b = -\zeta_a$) is twice bigger than the variance for a light sheet with one face coinciding with the in-focus plane (ζ_a or ζ_b null).

For very thin light sheet, the function $\arctan x$ of the variance (41) can be approximated by x. One obtains

$$\nu < \frac{\pi c^4 \xi^4 \tau^2 I^2 C M^2 \Delta\zeta}{64\sigma_0^2 f_\#^4 (1+M)^4} \tag{43}$$

In other words, taking into account (21), we have

$$\nu < \frac{\pi^3 c^4 \xi^3 \tau^2 I^2 C}{32\beta f_\#^3 (1+M)^3} \qquad \nu < \frac{\pi^3 c^4 \xi^2 \tau^2 I^2 C M^2 \Delta\zeta}{128\beta^2 f_\#^4 (1+M)^4} \tag{44}$$

The average μ is a constant that can be removed from the image. However, the shot noise associated with μ cannot be removed. This special shot noise will be further discussed in the next subsection.

The real "noise made by the other particles" is not expressed by the average μ, but by the standard deviation $\sqrt{\nu}$. Consequently, the noise is bounded by

$$N_p < \tau I c^2 \sqrt{\frac{\pi^3 \xi^3 C}{32\beta f_\#^3 (1+M)^3}} \qquad N_p < \frac{\tau I c^2 \xi M}{8\beta f_\#^2 (1+M)^2} \sqrt{\frac{\pi^3 C \Delta\zeta}{2}} \tag{45}$$

4.4 Background glow shot noise

Even though the background glow caused by the other particles can easily be removed from an image, the shot noise associated with it cannot be eliminated and constitutes a specific source of noise N_{gl}

$$N_{gl} = K_{ph}\sqrt{\mu} = K_{ph}\frac{c\xi\sqrt{\pi\tau IC\Delta\zeta}}{2f_{\#}(1 + M)} \tag{46}$$

where K_{ph} is the constant defined in subsection 4.1 for the photon shot noise.

5 Signal-to-noise ratio

5.1 Definition

The signal to noise ratio is defined by

$$\frac{S}{N} = \frac{S}{\sqrt{N_{ph}^2 + N_{th}^2 + N_p^2 + N_{gl}^2}} \tag{47}$$

Depending on the situation anyone of the four noises N_{ph}, N_{th}, N_p and N_{gl} can be dominant. In order to maximize the signal-to-noise ratio, let us assume that each of these noises is dominant in turn.

5.2 Dominant background glow shot noise

When the background glow shot noise N_{gl} is dominant, the signal-to-noise ratio S_0/N becomes

$$\frac{S_0}{N_{gl}} = \frac{cM^2}{2K_{ph}\beta f_{\#}(1 + M)}\sqrt{\frac{3\pi^3\tau I}{C\Delta\zeta(\pi^2M^2v^2\tau^2 + 12\beta^2\xi^2)}} \tag{48}$$

The signal-to-noise ratio S_0/N_{gl} can be maximized with respect to the exposure period τ. Indeed, the expression $\tau/(\pi^2M^2v^2\tau^2 + 12\beta^2\xi^2)$ reaches its maximum for

$$\tau_{opt} = \frac{2\sqrt{3}\beta}{\pi Mv}\xi \tag{49}$$

If β is chosen equal to $\sqrt{3}$, τ_{opt} equals τ_{max} of (26). With τ_{opt}, the signal-to-noise ratio expression S_0/N_{gl} becomes

$$\frac{S_0}{N_{gl}} = \frac{\pi c}{4K_{ph}f_{\#}(1 + M)}\sqrt{\frac{\sqrt{3}IM^3}{\xi C\Delta\zeta\beta^3v}} \tag{50}$$

The minimum particle image size σ_0 has been fixed by ξ at (21). Consequently the f-value cannot be arbitrarily chosen, but must give the corresponding σ_0. However, σ_0 is getting large for either high f-values (Fraunhofer diffraction) or low f-values (lens aberrations). Thus, to match the σ_0 fixed by ξ (21), there is the choice to take lower or higher f-values. On the other hand, to maximize the signal-to-noise ratio (as one can see in the above equation), the f-value should be small. Thus, the lens aberrations should be preferred to the Fraunhofer diffraction.

With the expression of $f_{\#}$ relative to the lens aberration (25), one obtains the column S_0/N_{gl} of Table 1. This table summarizes the qualitative variations of the signal-to-noise ratio with respect to the design parameters. The quantities are expressed in a logarithmic way. For example, the signal-to-noise ratio S_0/N_{ph} increases like $x^{+1/3}$ when the distance to the in-focus plane s decreases like s^{-1} (in other words, $S_0/N_{ph} \propto s^{-1/3}$).

Table 1: Logarithmic variations of the signal-to-noise ratio S_0/N

			$S_0/N_{\rm ph}$	$S_0/N_{\rm th}$	$S_0/N_{\rm gl}$	$S_0/N_{\rm p}$	
						$\Delta\zeta \gg 0$	$\Delta\zeta \approx 0$
s	-1	(distance to meas. plane)	$+1/3$	$+2/3$	$+1/3$	$+1/6$	0
M	$+1$	(magnification) $\quad M \gg 1$	$-5/6$	$-5/3$	$+1/6$	$+8/6$	$+1$
		$M \ll 1$	$+1/6$	$+1/3$	$+7/6$	$+11/6$	$+1$
ξ	$+1$	(pixel size)	$+5/6$	$+2/3$	$-1/6$	$-4/3$	-1
c	$+1$	(fill factor)	$+1$	$+1$	$+1$	$+0$	$+0$
I	$+1$	(illumination intensity)	$+1/2$	$+1$	$+1/2$	0	0
$\Delta\zeta$	-1	(light sheet thickness)	0	0	$+1/2$	0	$+1/2$
C	-1	(particle concentration)	0	0	$+1/2$	$+1/2$	$+1/2$
v	-1	(particle velocity)	$+1/2$	$+1$	$+1/2$	0	0
T	-1	(temperature)	0	$+1/2$	0	0	0

5.3 Dominant noise made by the other particles

When the noise $N_{\rm p}$ made by the other particles is dominant, the signal-to-noise ratio S_0/N tends to

$$\frac{S_0}{N_{\rm p}} > \frac{M^2\sqrt{6\pi}}{\sqrt{\xi C \beta f_\#(1+M)(\pi^2 M^2 v^2\tau^2 + 12\beta^2\xi^2)}} \qquad \frac{S_0}{N_{\rm p}} > \frac{2\sqrt{6}M}{\sqrt{\pi C \Delta\zeta M^2 v^2\tau^2 + 12\beta^2\xi^2}} \qquad (51)$$

The best signal-to-noise ratio is obtained for an exposure period τ equal to zero. Of course, if τ is too small, the other noises will be dominant. As the exposure period $\tau_{\rm opt}$ given in (49) is a sensible value between 0 and $\tau_{\rm max}$ of (26), let us assume that the best exposure time is $\tau_{\rm opt}$ in any situations (in any case, as long as τ is chosen in proportion to ξ/Mv, all the conclusions presented in this paper still hold). With this assumption, one obtains a closer expression for the signal S_0 of (28)

$$S_0 = \frac{\sqrt{6\pi}\,\xi I c^2 M}{8\beta f_\#^2(1+M)^2 v} \qquad (52)$$

and for the signal-to-noise ratio $S_0/N_{\rm p}$

$$\frac{S_0}{N_{\rm p}} > \frac{M^2}{2}\sqrt{\frac{\pi}{\xi^3 C\beta^3 f_\#(1+M)}} \qquad \frac{S_0}{N_{\rm p}} > \frac{M}{\beta\xi}\sqrt{\frac{\pi}{C\Delta\zeta}} \qquad (53)$$

When taking into account the expression (25) for $f_\#$, one eventually obtains the column $S_0/N_{\rm p}$ of Table 1

5.4 Other dominant noises

For PIV with low particle concentration C or possibly with low illumination intensity I, the dominant noise is no longer the noise made by the other particles or the background glow shot noise, but rather the photon shot noise or the thermal/read noise. One has when the photon shot noise is dominant and when the thermal/read noise is dominant

$$\frac{S_0}{N_{\rm ph}} = \frac{c}{K_{\rm ph}f_\#(1+M)}\sqrt{\frac{\sqrt{6\pi}\,\xi I M}{8\beta v}} \qquad \frac{S_0}{N_{\rm th}} = \frac{\sqrt{6\pi}\,I c M}{8K_{\rm th}\beta f_\#^2(1+M)^2 v\sqrt{kT}} \qquad (54)$$

The signal-to-noise ratio still could be improved for low f-value, i.e., for dominant lens aberrations. One obtains the column $S_0/N_{\rm ph}$ and $S_0/N_{\rm th}$ of Table 1. When these noises are dominant, there is an optimal magnification $M_{\rm opt}$. Indeed, the function $M/(1+M^6)$ has a maximum at

$$M_{\rm opt} = \left\lceil \frac{1}{5} \right\rceil^{1/6} \approx 0.58 \qquad (55)$$

Contrary to the other noises, an increase in the pixel size ξ results in an *increase* of signal-to-noise ratio. This is not very surprising, since larger pixels allow one to use an objective with lower f-value and to increase the exposure period. The interesting conclusion is that there exists an optimum value $\xi_{\rm opt}$ for the pixel size that balances the "camera noises" (photon noise and thermal/read noise) and the "particle noises" (background glow and noise made by the other particles).

6 Conclusion

The question addressed in this paper is: "What are the optimal quantities (related to the objective) that maximize the signal-to-noise ratio in a PIV setup?" To answer this question, we define the "signal" S_0 as the gray value of one pixel centered on an in-focus particle image. Depending on the application, any of the following noises can be dominant:

1. N_{ph}, fundamental photon shot noise

2. N_{th}, thermal and read noise

3. N_{gl}, background glow shot noise

4. N_p, noise made by the other particles

The following conclusions are read directly from Table 1. Conclusions 1 to 6 are expected by the common sense. Conclusions 7 to 9 are more interesting.

1. The fill factor c of the camera pixels should tend to its maximum 1.

2. The illumination intensity I should be chosen as high as possible.

3. The thickness $\Delta\zeta$ of the light sheet should be minimized.

4. The particle concentration C should be low.

5. The slow flows (small v) are easier to measure.

6. The camera should be actively cooled (low temperature T).

7. There is no optimal values for s, but there is a (slight) advantage to chose it the smaller possible, i.e., to have the objective the closer to the measurement plane.

8. If the photon shot noise or the thermal noise is dominant, there is an optimum magnification $M_{opt} \approx 0.58$. If the other noises are dominant, there is no optimum for M, but high values are preferred.

9. The pixel size ξ is generally given by the sensor technology, but image processing can "enlarge" it. Large values yield to better signal-to-noise ratio when the photon shot noise and the thermal/read noise are dominant. In the other case, small values give better results. This means that there exists an optimal pixel size ξ_{opt} that maximizes the total signal-to-noise ratio S_0/N. This optimum can be easily found by numerically computing S_0/N for different values of ξ and eventually selecting the best one.

Other important conclusions are:

• For a dominant background glow shot noise, there is an optimal exposure period τ_{opt}, i.e., that maximizes the signal-to-noise ratio [equation (49)]. For the other noises, the influence of τ is low and τ is bounded within 0 and τ_{max}. The consequence is that the same optimum exposure period τ_{opt} can be reasonably used.

• The f-value $f_\#$ of the objective has to be chosen as low as necessary to obtain a particle image large enough to fit the pixel size ξ by means of the lens aberrations [equation (25)].

This last conclusion is different from what is usually proposed in the literature, i.e., to enlarge the particle image by means of the Fraunhofer diffraction. A reason why the Fraunhofer diffraction is usually preferred may come from the lack of close and general expressions for lens aberrations. In this paper, the lens aberrations of a simple objective (comprising two doublets) have been empirically modeled from the results of many ray tracing simulations. This method has proved itself to be easy, accurate and effective.

Acknowledgment

References

[1] Adrian R J 1997 Dynamic ranges of velocity and spatial resolution of particle image velocimetry *Meas. Sci. and Tech.* (Bristol: Institute of Physics Publishing) **8** 12 p 1393

[2] Adrian R J and Yao C S 1985 Pulsed laser technique application to liquid and gaseous flows and the scattering power of seed materials *Appl Optics* **24** p 42

[3] Chételat O, Yoon S Y, Kim S K and Kim K C 2001 Design and construction of a miniature PIV (MPIV) system *Proc. ASV6, Asian symposium on visualization* (Busan, South Korea) p 163.1

[4] Chételat O, Yoon S Y and Kim K C 2001 Miniature PIV system (MPIV) with LED in-line illumination *Proc. PIV'01, 4th International symposium on particle image velocimetry* (Göttingen, Germany) p P1059.1

[5] Chételat O, Yoon S Y and Kim K C 2001 Design and construction of a miniature PIV (MPIV) system *KSME International Journal* **15** 12 p 1775

[6] Degrez G and Riethmuller M L 1994 Optical measurements *Measurement techniques in fluid dynamics, an introduction* (Belgium, Rhode-Saint-Genèse: von Karman Institute for Fluid Dynamics) Ch 6 p 229

[7] Dierickx B 2000 CMOS image sensors: concepts and limits *Short course at Photonics West 2000* (San Jose) also available at http://www.fillfactory.com/htm/technology/pdf/ pw00concepts.pdf and http://www.fillfactory.com/htm/technology/pdf/ pw00limits.pdf

[8] Huang H, Dabiri D and Gharib M 1997 On errors of digital particle image velocimetry *Meas. Sci. and Tech.* (Bristol: Institute of Physics Publishing) **8** 12 p 1427

[9] Jenkins F A and White H E 1981 *Fundamentals of Optics* (Singapore: Mc Graw-Hill Book Co)

[10] Lourenco L M 1996 Particle image velocimetry *Lecture Series 1996–03* (Belgium, Rhode-Saint-Genèse: von Karman Institute for Fluid Dynamics) pp 1–110

[11] Meinhart C D, Wereley S T and Gray M H B 2000 Volume illumination for two-dimensional particle image velocimetry *Meas. Sci. and Tech.* **11** p 809

[12] Michalski J 2001 What is telecentricity? http:// www.edmundoptics.com/techsup/ tsb/telecentricity.cfm (NJ/USA, Barrington: Edmund Industrial Optics)

[13] Olsen M G and Adrian R J 2000 Out-of-focus effects on particle image visibility and correlation in microscopic particle image velocimetry *Experiments in Fluids* (Springer-Verlag) **Suppl** p S166

[14] Ren K F, Lebrun D, Özkul C, Kleitz A, Gouesbet G and Gréhan G 1995 On the measurements of particles by imaging methods: theoretical and experimental aspects *Lecture Series 1996–03* (Belgium, Rhode-Saint-Genèse: von Karman Institute for Fluid Dynamics) pp 1–18

[15] Stanislas M and Monnier J C 1997 Practical aspects of image recording in particle image velocimetry *Meas. Sci. and Tech.* (Bristol: Institute of Physics Publishing) **8** 12 p 1417

[16] Westerweel J 1997 Fundamentals of digital particle image velocimetry *Meas. Sci. and Tech.* (Bristol: Institute of Physics Publishing) **8** 12 p 1379